

STABILIZED FORMULATION FOR ELECTROPHORETIC TRANSPORT PROBLEMS

Pablo A. Kler, Lisandro D. Dalcin and Rodrigo R. Paz

Centro Internacional de Métodos Computacionales en Ingeniería (CIMEC).

Instituto de Desarrollo Tecnológico para la Industria Química (INTEC).

Consejo Nacional de Investigaciones Científicas y Técnicas (CONICET).

Universidad Nacional del Litoral (UNL)

<http://www.cimec.org.ar>. E-mail: pkler@intec.unl.edu.ar

Keywords: Electrophoresis, Finite Element Simulation, SUPG, Shock capturing

Abstract. Electrophoresis consist in the relative motion of charged particles with respect to the surrounding liquid when an external electric field is applied. The magnitude of this relative velocity depends on the local magnitude of the electric field and the so-called electrophoretic mobility. Electrophoretic mobility represents the relationship between electric and hydrodynamic transport properties of the moving molecules. On the other side, the magnitude of the electric field depends on the electric conductivity of the solution and the electric potential differences applied at the inlets and outlets of fluid channels. This electric conductivity depends on the local concentration of ions, that also move due to the electrophoretic transport, which generates a strong coupling between mass transport and electric fields.

Solving electrophoretic transport problems numerically, and its coupling with fluid and electric problems, generates oscillations or instabilities in solutions that are directly related to the high values of the local Péclet number and the non null divergence of the migrative field. In order to surmount these difficulties a novel scheme of stabilization for this particular application is proposed. This stabilization technique is based on SUPG and shock capturing methods particularly adapted for this situation.

In order to demonstrate stabilization capability of the proposed formulation, some test are performed for 1D and 2D electrophoretic separations of molecules of biological interest.

1 INTRODUCTION

Electrophoresis is the relative motion of charged particles to the bulk or surrounding liquid. The magnitude of this relative velocity depends on the electrophoretic mobility. Differences on electrophoretic mobility result from balance between electric forces, and the hydrodynamic friction due to the viscosity of the surrounding solution. Electrophoretic separation techniques are the most common applications for electrophoresis, they consist in a separation method based on the differences on mobility of ions under an applied external electric field at the ends of capillaries or microchannels (Probstein, 2003).

Electrophoretic separations comprise a group of different techniques such as: capillary zone electrophoresis, isoelectric focusing, isotachopheresis, free flow electrophoresis, and capillary electrochromatography (Peng et al., 2008; Wu et al., 2008) that have been extensively used in chemical and biochemical analysis in a variety of scientific areas, such as genetics, molecular biology, pharmacology and environment monitoring, among others.

Electrophoretic separations are based on the electrokinetic phenomena that develop when electrolytic solutions interact with charged surfaces. Generally, most substances will acquire a surface electric charge when brought into contact with an aqueous (polar) medium. The effect of any charged surface in an electrolyte solution will be to influence the distribution of nearby ions in the solution. Ions of opposite charge to the surface (counterions) are attracted towards the surface while ions of like charge (coions) are repelled from the surface, this leads to the formation of an electric double layer (Hunter, 2001). The electric double layer is a region close to the charged surface in which there is an excess of counterions over coions to neutralize the surface charge. When an external electric field is applied in the axial direction of a channel, which is the case of electrophoretic separations, the electrical forces acting on excess ions drag the surrounding liquid and then electroosmotic flow (EOF) develops. Consequently, in modeling electrophoresis, results mandatory to include electric double layer and electroosmotic flow phenomena in order to obtain a comprehensive approach. This comprehensive approach, also has to take into account the different transport effects that interact in the electrophoretic transport as the diffusive, advective and the reactive effects as is usually done in the classical transport equation, but also the motion due to the electric forces has to be considered. The last is known as migrative effect.

The importance of model and simulate electrophoretic separations grounds on they can provide a more complete understanding of the fundamental of both physical and chemical process developed. Also, simulations are useful in order to optimize device designs and operation parameters, minimizing the risk of wasting time and money in flawed experiments or devices. The first mathematical model of electrophoresis was developed by Saville and Palusinski (1986). This 1D model is valid for monovalent analytes in a stagnant electrolyte solution, without considering (EOF). More complex models of conventional electrophoresis were later reported (Hruška et al., 2006; Thormann et al., 2007; Bercovici et al., 2009).

These simulations are useful for capillary electrophoresis where the system is inherently 1D due to the uniform section of the capillary and the high aspect ratio. These kind of simulations can be done without any limitations by using 1D finite differences as is the case of cited works. In the case of electrophoretic separations developed on microfabricated chips there exist multiple channels with different sections and such a system requires more complex simulation domains. These simulations started with works of Patankar and Hu (1998) and Ermakov et al. (1998) by using 2D finite element method (FEM). Chatterjee (2003) developed a 3D finite volume model to study several applications in microfluidics, including isoelectric focusing. More

recently, [Barz \(2009\)](#) developed a fully coupled model for electrokinetic flow and migration in microfluidic devices employing 2D FEM, other important related works are those of [Shim et al. \(2007\)](#) and [Albrecht et al. \(2007\)](#) in 2D domains by using flux corrected transport method.

Numerical simulations of electrophoretic separations in microfluidic chips represent a challenging problem from the computational point of view. Both the large difference among the relevant length scales involved and the multiphysics nature of the problem, lead to numerical difficulties: multiple nonlinear problems, excessive number of degrees of freedom, and ill-conditioning global matrices due to the high aspect ratios. Therefore, the implementation of parallel computations and advanced preconditioning, such as domain decomposition techniques, are crucial for the achievement of accurate numerical results and low computation times. Parallel computations and domain decomposition techniques in modeling electrokinetic flow and mass transport have not been extensively explored. [Tsai et al. \(2005\)](#) presented a 2D parallel finite volume scheme to solve EOF in L-shaped microchannels. 3D simulations of electrophoretic processes employing parallel calculations were performed by [Chau et al. \(2008\)](#) for free flow electrophoresis using finite difference method, and by [Kler et al. \(2009, 2011\)](#) for electroosmotic flow, capillary zone electrophoresis, isoelectric focusing and two dimensional electrophoresis using 3D FEM.

It is well known that, when solving transport problems by using FEM some stabilization method is required in order to avoid oscillations or instabilities in numerical solutions ([Donea and Huerta, 2003](#)). Generally, these undesirable effects are directly related to the high values of the local Péclet number. In solving electrophoretic transport problems not only the local Péclet value is important, also the strong coupling with fluid and electric problems generates a non null divergence advective field for the migration effect. When the migration field acts on a non uniform concentration field, generally results in high gradients or even discontinuities in the concentration of different ions. This situation increase the need of a stabilization method.

One of the most popular methods to stabilize FEM formulations for transport problems is the streamline upwind Petrov - Galerkin (SUPG) method originally proposed by [Hughes and Tezduyar \(1984\)](#) (see also [Hughes et al. \(1987\)](#)). A more recent work of [Tezduyar et al. \(1992\)](#) is based on the addition of a factor τ that depends on the local length scales and values of Péclet and Courant numbers. This formulation was aimed to avoid oscillations in solving scalar advective-diffusive equations with an advective dominant term. The non null divergence of the advective field due to the migration term generates high concentration gradients in the transported ionic species. In order to stabilize this kind of solutions in the concentration field, Shock Capturing (SC) method was proposed initially by [Hughes and Mallet \(1986\)](#). More recently, [Tezduyar and Senga \(2004\)](#) proposed including the δ factor to scale the SC term as a function of the relative magnitude of the concentration gradients.

In this work we present a novel stabilization scheme for the electrophoretic transport equations, based on SUPG and SC methods particularly adapted. This scheme involves adapted forms for the calculation of the SUPG and SC terms and the τ and δ expressions.

2 GOVERNING EQUATIONS

This section describes the mathematical model for electrophoretic separations. The model includes the fluid dynamics, electric field, mass transport, chemical reactions, and the coupling between all of these fields.

2.1 Flow field

In the framework of continuum fluid mechanics, fluid velocity u and pressure p are governed by the following equations (Probstein, 2003; Li, 2004):

$$-\nabla \cdot \mathbf{u} = 0, \quad (1)$$

$$\rho \left(\frac{\partial \mathbf{u}}{\partial t} + \mathbf{u} \cdot \nabla \mathbf{u} \right) = \nabla \cdot (-p\mathbf{I} + \mu(\nabla \mathbf{u} + \nabla \mathbf{u}^T)) + \rho \mathbf{g} + \rho_e \mathbf{E}. \quad (2)$$

Equation 1 expresses the conservation of mass for incompressible fluids. Equation 2 expresses the conservation of momentum for Newtonian fluids of density ρ , viscosity μ , subjected to gravitational field of acceleration \mathbf{g} and electric field strength \mathbf{E} . The last term on the right hand side of Equation 2 represents the contribution of electrical forces to the momentum balance, where $\rho_e = F \sum_j z_j c_j$ is the electric charge density of the electrolyte solution, obtained as the summation over all type- j ions, with valence z_j and concentration c_j , and F is the Faraday constant.

2.2 Electric field

The relationship between electric field and charge distributions in the fluid of permittivity ϵ is given by

$$\epsilon \nabla \cdot \mathbf{E} = \rho_e. \quad (3)$$

Modeling electrophoresis problems demands special considerations on the electric field, since it involves different contributions in the flow domain, and is strongly affected by the presence of non-uniform electrolyte concentrations. Here we describe the computation of the electric field, as well the hypothesis included to simplify numerical calculations. For this purpose, a (η, τ) wall-fitted coordinate system is used, where η and τ are, respectively, the coordinates normal and tangent to the solid boundaries.

The first contribution to the electric field comes from the presence of electrostatic charges at solid-liquid interfaces. The interfacial charge has associated an electric potential ψ that decreases steeply in η -direction due to the screening produced by counterions and other electrolyte ions in solution. The value of ψ at the plane of shear depends on the wall - solution interactions and it is known as the electrokinetic potential ζ . Also in this modeling, ζ is allowed to vary smoothly along the τ -direction on a length scale L in the order of 1 *cm* which is referred to channel or capillary lengths. Nevertheless, since $\zeta/\lambda_D \gg \zeta/L$, the variation of ψ with τ is disregarded and ψ is assumed to vary with η only.

There is also a potential ϕ in the flow domain, which comes from the potential difference $\Delta\phi$ externally applied to drive electrophoresis and/or induce EOF. As the channel walls are supposed perfectly isolating, there are no components of the applied field normal to the wall, and ϕ varies in τ -direction only. Therefore the total electric potential may be written as

$$\Phi(\eta, \tau) = \psi(\eta) + \phi(\tau). \quad (4)$$

This superposition is valid if the EDL retains its equilibrium charge distribution when the electrolyte solution flows. The approximation is part of the standard electrokinetic model (Hunter, 2001) and holds if the applied electric field ($\sim \Delta\phi/L$) is small in comparison with

the EDL electric field ($\sim \zeta/\lambda_D$), which is normally the case encountered in practice. Introducing the electric field $\mathbf{E} = -\nabla\Phi$ into Equation 3 leads to the following expression,

$$\frac{\partial^2\psi}{\partial\eta^2} + \frac{\partial^2\phi}{\partial\tau^2} = -\frac{\rho_e}{\epsilon}. \quad (5)$$

The second term on the left hand side of Equation 5 is non-null in electrophoresis problems because the presence of concentration gradients in the fluid induces a variation of $\frac{\partial\phi}{\partial\tau}$ along the channel. However, $\frac{\partial^2\phi}{\partial\tau^2}$ is several orders of magnitude lower than $\frac{\partial^2\psi}{\partial\eta^2}$ (see also MacInnes (2002); Sounart and Baygents (2007); Craven et al. (2008)), which allows one to split the computation of the electric field in two parts, as explained below.

2.2.1 Electric double layer

According to the previous analysis, the EDL potential is governed by

$$\frac{\partial^2\psi}{\partial\eta^2} = -\frac{\rho_e}{\epsilon}. \quad (6)$$

Nevertheless, computational requirements are very large when a whole electrophoretic device is modeled. In this sense, here we simplify the calculation of the EOF by introducing the so-called thin EDL approximation (Brunet and Adjari, 2004; Berli, 2008): EOF is regarded as an electrically induced slip velocity in the direction of the applied electric field, the magnitude of which is given by Helmholtz-Smoluchowski equation:

$$\mathbf{u}_{eo} = -\frac{\epsilon_0\epsilon_r\zeta_w\mathbf{E}}{\mu} \quad (7)$$

This approximation also implies that $\rho_e \approx 0$ in the fluid outside the EDL, meaning that the last term on the right-hand side of Equation 2 is negligible. Thus the electroosmotic velocity enters the hydrodynamic field as a boundary condition, which significantly reduces computational demands. The simplification is appropriate taking into account that $\lambda_D \approx 1 - 10 \text{ nm}$, while cross-sectional channel or capillary dimensions are $20 - 200 \mu\text{m}$.

2.2.2 Bulk fluid

Given the considerations made above, the electric potential $\phi(\tau)$ has to be calculated from the charge conservation equation in steady state (Probstein, 2003):

$$\nabla \cdot \left(-\sigma\nabla\phi - F \sum_{j=1}^N z_j D_j \nabla c_j + \rho_e \mathbf{u} \right) = 0 \quad (8)$$

where D_j is the diffusion coefficient of the specie j , N is the number of different ionic species present in the electrolyte solution, and σ is the electrical conductivity, given by:

$$\sigma = F \sum_{j=1}^N z_j^2 \Omega_j c_j \quad (9)$$

where Ω_j is the ionic mobility. In fact, the terms between brackets in Equation 8 constitute the electric current density i , which accounts for the ion fluxes due to fluid convection, electrical forces, and Brownian diffusion. Finally one may note that Equation 8 reduces to $\frac{\partial^2 \phi}{\partial \tau^2} = 0$ (Laplace equation for the applied potential) only if electrolyte concentrations and mobilities are perfectly uniform and stagnant.

2.3 Mass transport and chemistry

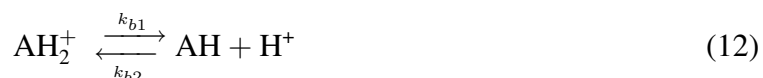
The mass transport of weakly concentrated sample molecules and buffer electrolyte constituents can be modelled by a linear superposition of migrative, convective and diffusive transport mechanisms, plus a source term due to chemical reactions. In a non-stationary mode, the concentration of each j -type species, is governed by (Probstein, 2003):

$$\frac{\partial c_j}{\partial t} + \nabla \cdot (-z_j \Omega_j \nabla \phi c_j + \mathbf{u} c_j - D_j \nabla c_j) - r_j = 0 \quad (10)$$

where r_j is the reaction term. Different electrolytes (acids, bases and ampholytes), analytes, and particularly the hydrogen ion have to be considered. In electrolyte chemistry the processes of association and dissociation are much faster than the transport electrokinetic processes, hence, it is a good approximation to adopt chemical equilibrium constants to model the reactions of weak electrolytes (Arnaud et al., 2002), while strong electrolytes are considered as completely dissociated.

2.3.1 Acid-base reactions

For the general case, reactions associated to an ampholyte AH are



where k_{a1} , k_{b1} are the dissociation rates, and k_{a2} , k_{b2} are the association rates for the acidic and basic reactions respectively. Then the equilibrium state is characterized by,

$$\frac{k_{a2}}{k_{a1}} = \frac{[A^-][H^+]}{[AH]} = K_a \quad (13)$$

$$\frac{k_{b2}}{k_{b1}} = \frac{[AH][H^+]}{[AH_2^+]} = K_b \quad (14)$$

where K_a and K_b are the equilibrium constants, for the acidic and basic reactions respectively, and the square brackets represent concentration in mol m^{-3} , of the given specie. The corresponding expressions of r_j are obtained as follows,

$$r_{A^-} = -k_{a1}[A^-][H^+] + k_{a2}[AH] \quad (15)$$

$$r_{AH} = k_{a1}[A^-][H^+] - k_{a2}[AH] - k_{b1}[AH][H^+] + k_{b2}[AH_2^+] \quad (16)$$

$$r_{AH_2^+} = k_{b1}[AH][H^+] - k_{b2}[AH_2^+] \quad (17)$$

$$r_{H^+} = -k_{a1}[A^-][H^+] + k_{a2}[AH] - k_{b1}[AH][H^+] + k_{b2}[AH_2^+]. \quad (18)$$

In Equation 18 the water dissociation term is not included due to the fact that this reaction is several orders of magnitude faster than reactions 11 and 12 (Arnaud et al., 2002), then $[OH^-]$ can be calculated directly as

$$[OH^-] = \frac{K_w}{[H^+]} \quad (19)$$

where $K_w = 10^{-14} \text{ mol}^2\text{m}^{-6}$, is the dissociation constant for pure water at 25°C.

2.3.2 Effective charge and mobility of analytes

When the concentration of analytes is much lower than that of buffer constituents, its effect on the pH is negligible. In these cases, considering all ionic species represents a high computational cost. However the influence of pH on the analytes must be taking into account. Thus the transport equation of these analytes includes $r_j = 0$, and the product $z_j\Omega_j$ as a function of pH. For example, if the specie is an ampholyte that obeys a reaction scheme like the one shown in Equations 11 and 12, $z_j\Omega_j$ is included in Equation 10 as an effective charge-mobility product ($z_{eff(j)}\Omega_{eff(j)}$; Chatterjee (2003)). This product is calculated as $(\alpha_0 - \alpha_2)\Omega_j$, where α_0 and α_2 are the degrees of dissociation of anionic and cationic forms, respectively, which are written in terms of $[H^+]$ as,

$$\alpha_0 = \frac{\frac{K_a K_b}{[H^+]^2}}{1 + \frac{K_b}{[H^+]} + \frac{K_a K_b}{[H^+]^2}} \quad (20)$$

$$\alpha_2 = \frac{1}{1 + \frac{K_b}{[H^+]} + \frac{K_a K_b}{[H^+]^2}} \quad (21)$$

Therefore the governing equation for concentration of the j -specie in the sample plug results,

$$\frac{\partial c_j}{\partial t} + \nabla \cdot [-(\alpha_0 - \alpha_2)\Omega_j \nabla \phi c_j + \mathbf{u}c_j - D_j \nabla c_j] = 0 \quad (22)$$

where it is observed that the physical motion of analytes is coupled to the degree of dissociation at a given pH.

3 SUPG AND SHOCK CAPTURING FORMULATIONS

In order to solve the mass transport problem, Equation 10 was used. The FEM formulation for this equation, by using the Galerkin method, integration by parts, and the piecewise linear function space V_h , is:

find c_j^h , such as $c_j^h, v_h \in V_h$ and

$$\int_{\Omega^h} v_h \frac{\partial c_j^h}{\partial t} + v_h \nabla \cdot (-z_j \Omega_j^h c_j^h \nabla \phi_h + c_j^h \mathbf{u}_h) - v_h r_j + \nabla v_h \cdot D_j \nabla c_j^h \, d\Omega^h = 0 \text{ in } \Omega^h$$

$$\begin{aligned} c_j^h &= c_{j\Gamma} \text{ at } \Gamma_D \\ \frac{\partial c_j^h}{\partial n} &= 0 \text{ at } \Gamma_N \\ \frac{\partial c_j^h}{\partial n} &= \Phi_j \text{ at } \Gamma_R \end{aligned} \tag{23}$$

for $j = 1, 2, 3, \dots, N$, where $\Gamma = \Gamma_D \cup \Gamma_N \cup \Gamma_R$, $\Gamma_D \cap \Gamma_N \cap \Gamma_R = \emptyset$. When this equation is implemented numerically, several aforementioned problems on stability due to the high value of the Péclet number arises (Donea and Huerta, 2003), for this equation this dimensionless number can be written, for the specie j , as

$$Pe_j = \frac{L \parallel (-z_j \Omega_j^h \nabla \phi_h + \mathbf{u}_h) \parallel}{D_j} \tag{24}$$

where L is a characteristic length. In order to avoid these instabilities, SUPG and SC are proposed following previous works of Tezduyar and Osawa (2000) and Tezduyar and Senga (2004), respectively. The final FEM equation implemented for the electrophoretic mass transport equation is

$$\begin{aligned} &\int_{\Omega^h} v_h c_{j,t}^h - v_h \nabla \cdot (z_j \Omega_j^h \nabla \phi_h c_j^h - \mathbf{u}_h c_j^h) - v_h r_j \, d\Omega^h + \int_{\Omega^h} \nabla v_h \cdot D_j \nabla c_j^h \, d\Omega^h - \\ &\sum_{e=1}^{nel} \int_{K^e} \tau_{supg_j} (z_j \Omega_j^h \nabla \phi_h - \mathbf{u}_h) \cdot \nabla v_h (c_{j,t}^h - r_j - \nabla \cdot (z_j \Omega_j^h \nabla \phi_h c_j^h - \mathbf{u}_h c_j^h)) \, d\Omega^h \\ &+ \sum_{e=1}^{nel} \int_{K^e} \delta_{shock_j} \nabla v_h \nabla c_j^h \, d\Omega^h = 0 \end{aligned} \tag{25}$$

for $j = 1, 2, 3, \dots, N$, where nel is the number of elements of T_h , and $c_{j,t}^h$ corresponds to the discrete temporal derivative, following a general Crank-Nicolson scheme with real parameter θ , such as $0 \leq \theta \leq 1$. Diffusion term in the SUPG integral vanishes for lineal elements, and τ_{supg} calculate for each specie j as follows

$$\tau_{s1} = \frac{\Delta t}{2\theta} \tag{26}$$

$$\tau_{s2_j} = \frac{h_{supg_j}}{2 \parallel (-z_j \Omega_j^h \nabla \phi_h + \mathbf{u}_h) \parallel} \tag{27}$$

$$\tau_{s3_j} = \frac{h_{supg_j}^2}{12D_j} \tag{28}$$

$$\tau_{s4_j} = \frac{1}{\nabla \cdot (-z_j \Omega_j^h \nabla \phi_h + \mathbf{u}_h)} \tag{29}$$

where

$$h_{\text{supg}_j} = \nabla v_h \cdot \left(\frac{(-z_j \Omega_j^h \nabla \phi_h + \mathbf{u}_h)}{\|(-z_j \Omega_j^h \nabla \phi_h + \mathbf{u}_h)\|} \right) \quad (30)$$

finally, if $\|(-z_j \Omega_j^h \nabla \phi_h + \mathbf{u}_h)\| > \text{tol}_{\text{supg}}$:

$$\tau_{\text{supg}_j} = \left(\frac{1}{\tau_{s1}^2 + \tau_{s2}^2 + \tau_{s3}^2 + \tau_{s4}^2} \right)^{\frac{1}{2}} \quad (31)$$

and, if $\|(-z_j \Omega_j^h \nabla \phi_h + \mathbf{u}_h)\| \leq \text{tol}_{\text{supg}}$:

$$\tau_{\text{supg}_j} = 0 \quad (32)$$

where tol_{supg} is a predefined tolerance depending on the smallest scales of time and longitude involved in the problem.

Also δ_{shock} calculate for each specie j as:
if $\|\nabla c_j^h\| > \text{tol}_{\text{shock}}$,

$$\delta_{\text{shock}_j} = \frac{h_{\text{shock}_j}}{2} \|(-z_j \Omega_j^h \nabla \phi_h + \mathbf{u}_h)\| \left(\frac{\|\nabla c_j^h\| h_{\text{shock}_j}}{c_{\text{ref}_j}^h} \right)^2, \quad (33)$$

and, if $\|\nabla c_j^h\| \leq \text{tol}_{\text{shock}}$:

$$\delta_{\text{shock}_j} = 0 \quad (34)$$

where, $c_{\text{ref}_j}^h$ is a reference value for the concentration of the specie j , and

$$h_{\text{shock}_j} = \nabla v_h \cdot \left(\frac{\nabla c_j^h}{\|\nabla c_j^h\|} \right) \quad (35)$$

where $\text{tol}_{\text{shock}}$ is a predefined tolerance depending on the smallest scales of concentration and longitude involved in the problem.

4 NUMERICAL EXAMPLES

In this section, numerical tests and application examples are presented. The first example is a 1D test for electrophoretic transport in capillaries, in which are shown the different results obtained when different stabilization schemes are used. Following, a 2D application example is presented where the different advective fields acts on the transported sample in different directions for different specie.

4.1 1D test: capillary electrophoresis

In this first test we shall demonstrate the effects on considering the SUPG and SC terms in advective dominant problems, as is the case of the separation by capillary electrophoresis (CE).

In an CE assay, an electric potential difference is applied at the ends of a capillary tube or a microchannel in order to obtain a longitudinal electric field. This electric field exerts forces on the charged molecules in solution resulting in different electrophoretic velocities enabling the separation due to this difference.

In this example, two acidic specie (Hydrochloric acid and Tetraphenylborate) are separated electrophoretically, using a low concentrated buffer of tris(hydroxymethyl)-aminoetane (TRIS) and Acetic Acid. Physicochemical properties of buffer and analytes are listed in Table 1. Initial conditions for samples and buffer constituents are shown in Fig. 1.

Component	pK_a	pK_b	Mobility (m^2/Vs)	Diffusivity (m^2/s)	Initial concentration
Hydrochloric acid	-2.0	-	$7.91 \cdot 10^{-8}$	$2.03 \cdot 10^{-9}$	5 mM
Tetraphenylborate	5.0	-	$1.80 \cdot 10^{-8}$	$4.60 \cdot 10^{-10}$	5 mM
TRIS	-	8.08	$2.95 \cdot 10^{-8}$	$7.60 \cdot 10^{-10}$	75 mM
Acetic acid	4.76	-	$4.20 \cdot 10^{-8}$	$1.08 \cdot 10^{-9}$	380 μM

Table 1: Physicochemical properties of buffer constituents and analytes.

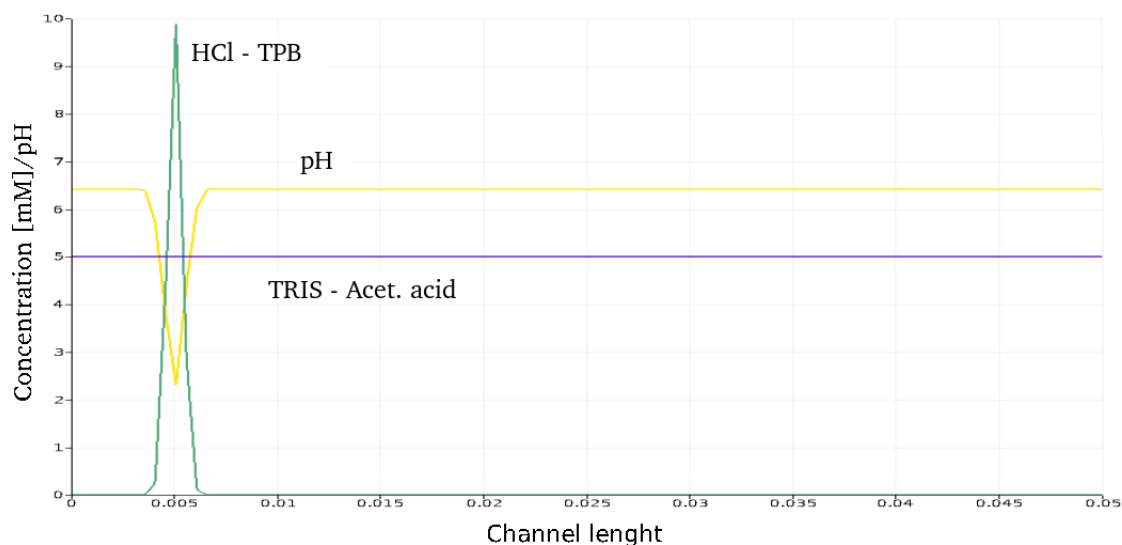


Figure 1: Initial conditions for samples and buffer constituents.

Due to the low concentration of buffer components, relative to the samples, samples and their motion affects the local physicochemical properties of the electrolyte solution. This mean, that the local presence of sample in a region of the capillary, affects both the electric conductivity (Equation 9) and the local acid - base equilibrium (pH of the solution, as is shown in Figure 1). The first affect the local values of the electric field, and the second alters the effective mobility of the samples (see Equations 20 and 21), generating a dual strong coupling between the numerical solutions of the electric field and the transport equations (Equations 8 and 10). This situation can be inferred from Figure 2.

In order to carry out the test, a 3000 V difference of electric potential is exerted between the ends of a 5 cm long capillary, filled with the electrolytic solution. As was mentioned, this potential difference, generates an electric field that exerts electric forces on samples that enables

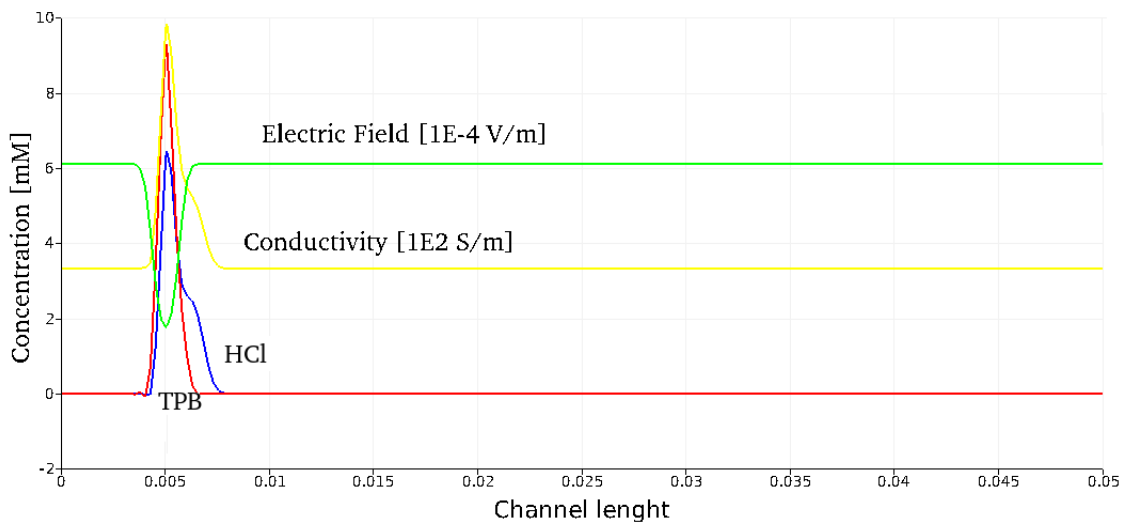


Figure 2: Coupling between sample concentrations, conductivity, and electric field.

the separation due to the difference on effective mobilities. Mobility of Hydrochloric acid is higher than the one of Tetraphenil borate due to the local pH values, and as a consequence the displacement of Hydrochloric acid is also higher.

Figure 3 shows the sample concentration distribution at two different times, and the effect on these distribution of adding of stabilization terms. It is clear that the stabilization terms contribute to eliminate the non-physical undesired oscillations on numerical solutions.

4.2 2D test: free flow electrophoresis

In this test we demonstrate the effectiveness of the proposed method for simulate electrophoretic transport with conjugation of classic advective field (fluid velocity) and migration field in variable directions. In this case an electrophoretic separation process is simulated by using free flow electrophoresis (FFE) method.

Free flow electrophoresis consist in a continuous technique for electrophoretic separations. These methods provide bands across the separation chamber and thus a continuous supply of separated components at the exit of the chamber. In FFE, charged particles are injected into a liquid carrier with an electric field applied perpendicular to the flow direction. Particles are deflected from the flow streamlines at an angle arranged by the vector composition of the fluid advection and the migration (determined by the sample mobility and the applied electric field strength). Sample compounds with different electrophoretic mobility have different deflections and can be collected separately at the end of the separation area.

In this example, two aminoacids from a single flow are separated in the streams and redirected to two individual channels. Physicochemical properties of analytes are listed in Table 2.

Component	pK_a	pK_b	Mobility (m^2/Vs)	Diffusivity (m^2/s)	Initial concentration
Aspartic Acid	2.28	3.90	$2.83 \cdot 10^{-8}$	$7.31 \cdot 10^{-9}$	1 mM
Lysine	9.12	10.79	$2.70 \cdot 10^{-8}$	$6.98 \cdot 10^{-10}$	1 mM

Table 2: Physicochemical properties of buffer constituents and analytes.

In order to develop the FFE, a 750 V electric potential difference is applied at the exit chan-

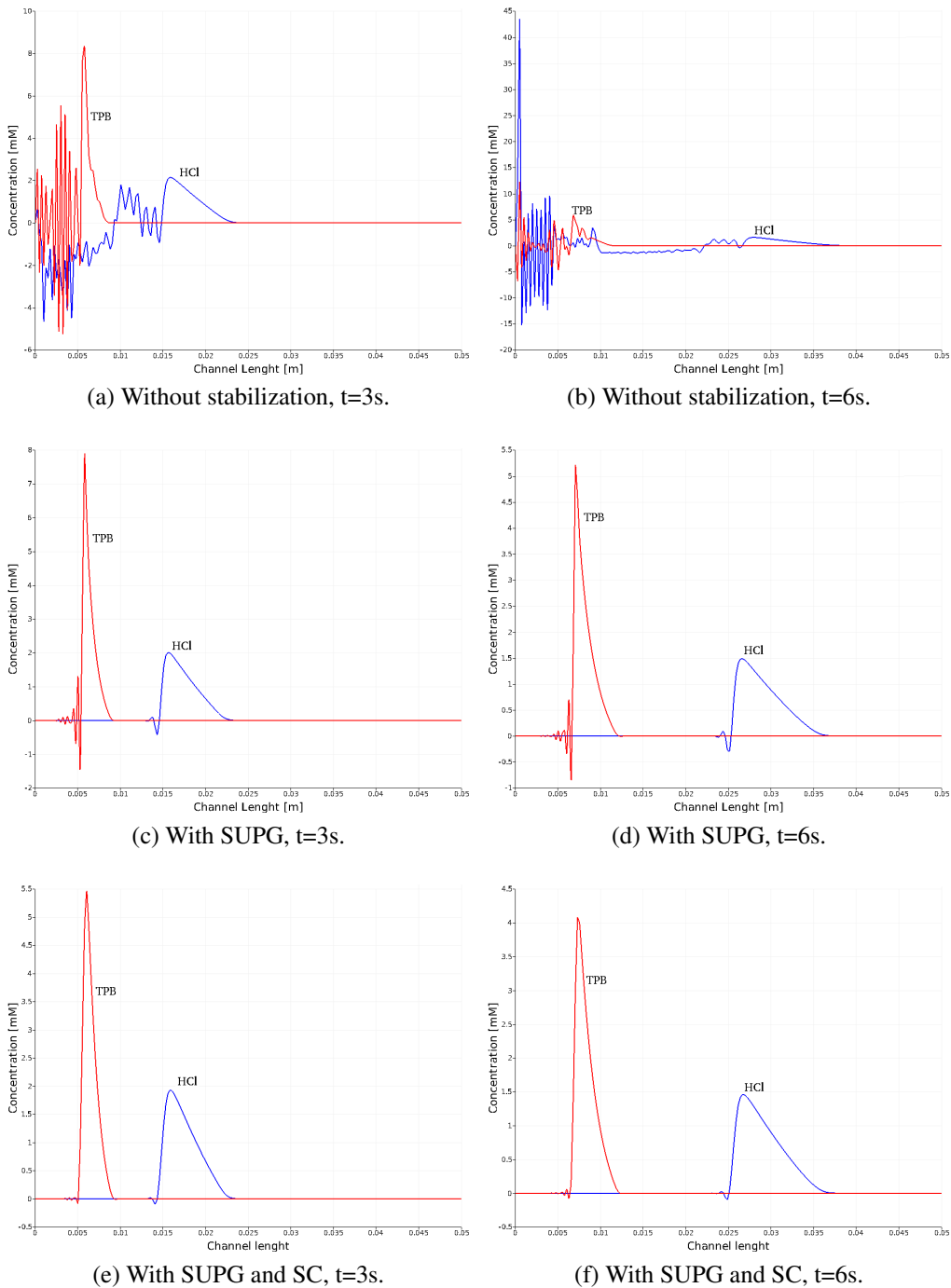


Figure 3: Stationary state results for the capillary ITP.

nels and a velocity field is developed by imposing an inlet velocity of 1.0 cm/s. Geometry of the FFE device, electric potential, electric field and field lines are shown in Figure 4. The pressure field, velocity field, and the streamlines for velocity are shown in Figure 5. From field lines on Figure 4 and streamlines from Figure 5 can be inferred the superposition of the two effects (migrative and advective respectively) with variable directions. The resulting motion of the substances will be the superposition of these effects (plus the dispersion due to the diffusion) resulting in the separation of the aminoacids.

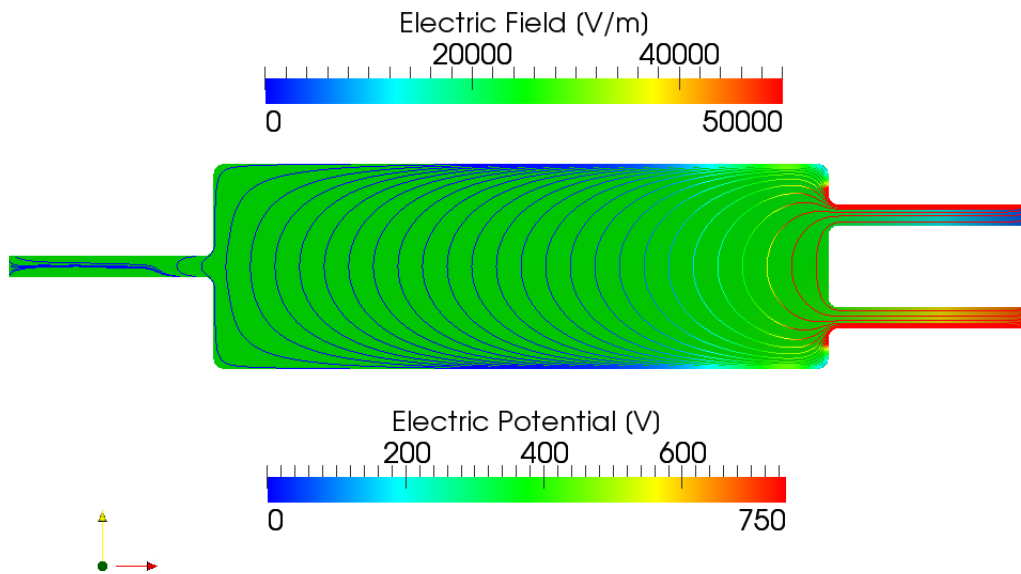


Figure 4: Electric potential, electric field and field lines.

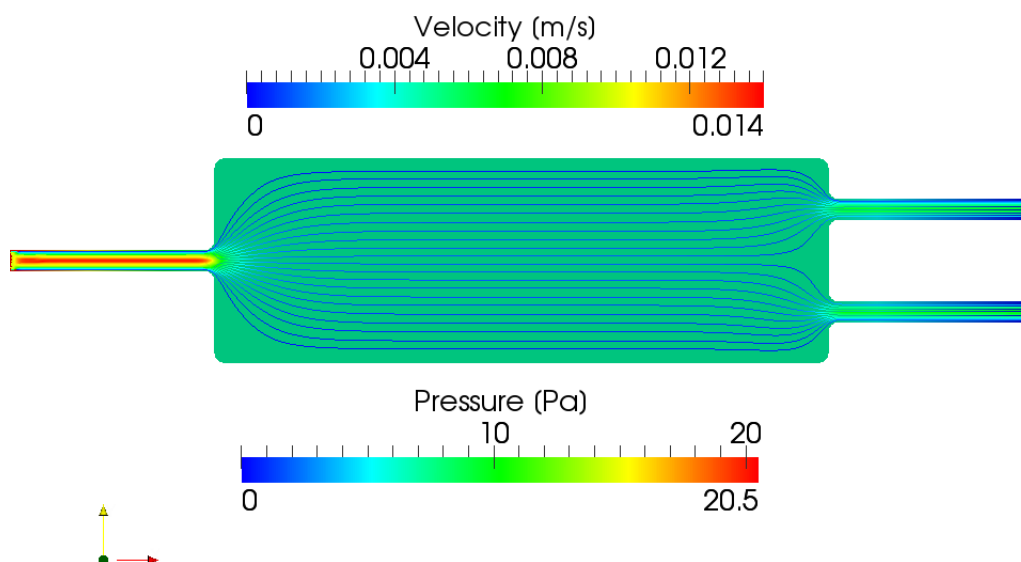


Figure 5: Pressure, velocity and streamlines.

Due to the difference on the dissociation points, the net charge of the Aspartic Acid is negative and the net charge of Lysine is positive, generating the electrophoretic separation. Due to this properties, the Aspartic Acid tends to move downwards to the positive potential region, and

then enters to the bottom channel. Similarly, due to its negative charge, Lysine moves upward following the electric field, and finally entering to the upper channel. Aspartic Acid and Lysine concentration distributions at different times are shown in Figure 6.

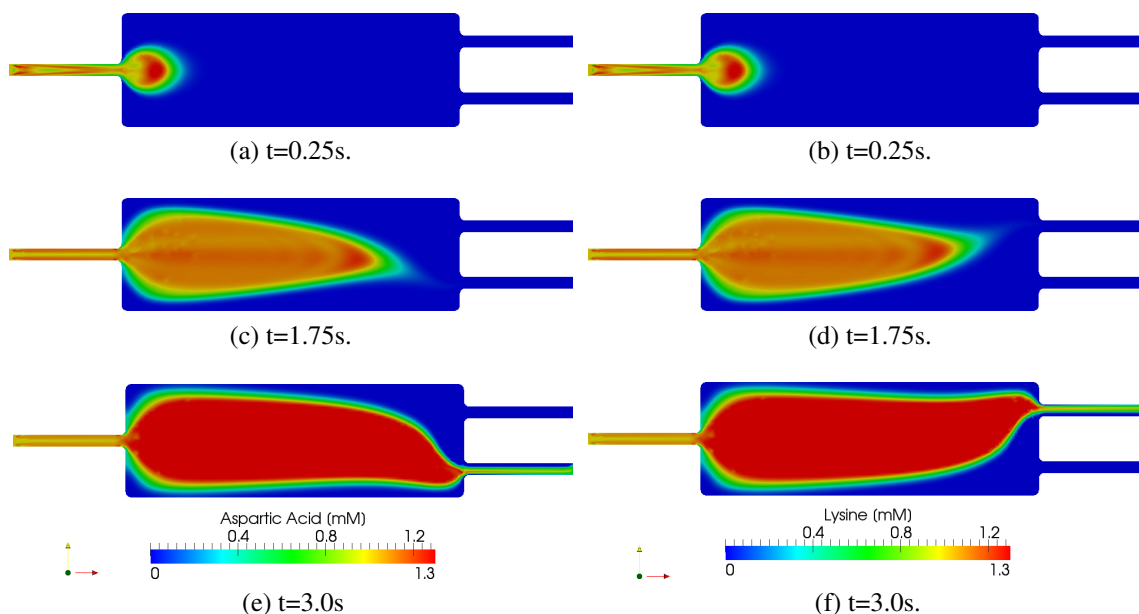


Figure 6: Aspartic Acid and Lysine distribution at different times.

5 CONCLUDING REMARKS

In this work we have presented a novel stabilization scheme aimed to electrophoretic transport equations solved numerically by using FEM. This stabilization scheme is based on the well known SUPG and SC methods developed for scalar equations. We proposed novel expressions for the SUPG and SC terms for the FEM formulations of the vectorial concentration field, and the values for the factors τ_{SUPG} and δ_{shock} , for each specie, taking into account the different effects involved in the electrophoretic process.

Two application examples were presented in order to show the effectiveness of the method. In the first case the effect of adding stabilization terms clearly shows the benefits in order to eliminate the non physical oscillations that typically show numerical solutions of advective dominant problems as is the case of the electrophoretic transport.

The second example shows a numerical simulation of a typical application of electrophoretic separation in which the fluid velocity and the electric field have variable directions. In this case the stabilization method provides benefits for the composition of both fluid and electric advective effects which is a challenging situation in numerical simulations of electrophoretic separations.

6 ACKNOWLEDGMENTS

This work has received financial support from *Consejo Nacional de Investigaciones Científicas y Técnicas* (CONICET, Argentina, grant PIP 5271/05), *Universidad Nacional del Litoral* (UNL, Argentina, grant CAI+D 2009 65/334 and 65/238), *Agencia Nacional de Promoción Científica y Tecnológica* (ANPCyT, Argentina, grants PICT 01141/2007, PICT 0270/2008, PICT-1506/2006).

REFERENCES

- Albrecht J.W., El-Ali J., and Jensen K.F. Cascaded free-flow isoelectric focusing for improved focusing speed and resolution. *Anal. Chem.*, 79:9364 – 9371, 2007.
- Arnaud I., Josserand J., Rossier J., and Girault H. Finite element simulation of off-gel buffering. *Electrophoresis*, 23:3253–3261, 2002.
- Barz D.P. Comprehensive model of electrokinetic flow and migration in microchannels with conductivity gradients. *Microfluid. Nanofluid.*, 7(2):249 –265, 2009.
- Bercovici M., Lele S.K., and Santiago J.G. Open source simulation tool for electrophoretic stacking, focusing, and separation. *J. Chromatogr. A*, 1216:1008 – 1018, 2009.
- Berli C.L.A. Equivalent circuit modeling of electrokinetically driven analytical microsystems. *Microfluid. Nanofluid.*, 4(5):391 – 399, 2008.
- Brunet E. and Adjari A. Generalized Onsager relations for electrokinetic effects in anisotropic and heterogeneous geometries. *Phys. Rev. E*, 69(1):016306, 2004.
- Chatterjee A. Generalized numerical formulations for multi-physics microfluidics-type applications. *J. Micromech. Microeng.*, 13:758–767, 2003.
- Chau M., Spiteri P., Guivarich R., and Boisson H. Parallel asynchronous iterations for the solution of a 3d continuous flow electrophoresis problem. *Comput. Fluid.*, 37(9):1126–1137, 2008.
- Craven T.J., Rees J.M., and Zimmerman W.B. On slip velocity boundary conditions for electroosmotic flow near sharp corners. *Phys. Fluids*, 20(4):043603, 2008.
- Donea J. and Huerta A. *Finite Element Methods for Flow Problems*. Wiley Online Library, 2003.
- Ermakov S., Jacobson S., and Ramsey J. Computer simulations of electrokinetic transport in microfabricated channel structures. *Anal. Chem.*, 70(21):4494–4504, 1998.
- Hruška V., Jaros M., and Gaš B. Simul 5 - free dynamic simulator of electrophoresis. *Electrophoresis*, 27:984–991, 2006.
- Hughes T., Franca L., and Mallet M. A new finite element formulation for computational fluid dynamics: Vi. convergence analysis of the generalized supg formulation for linear time-dependent multidimensional advective-diffusive systems. *Comput. Method. Appl. M.*, 63(1):97–112, 1987.
- Hughes T. and Mallet M. A new finite element formulation for computational fluid dynamics: Iv. a discontinuity-capturing operator for multidimensional advective-diffusive systems* 1. *Comput. Method. Appl. M.*, 58(3):329–336, 1986.
- Hughes T. and Tezduyar T. Finite element methods for first-order hyperbolic systems with particular emphasis on the compressible euler equations. *Comput. Method. Appl. M.*, 45(1-3):217–284, 1984.
- Hunter R. *Foundations of Colloid Science*. Oxford University Press, second edition, 2001.
- Kler P., Berli C., and Guarnieri F. Modeling and high performance simulation of electrophoretic techniques in microfluidic chips. *Microfluidics and Nanofluidics*, 10(1):187–198, 2011.
- Kler P.A., López E.J., Dalcín L.D., Guarnieri F.A., and Storti M.A. High performance simulations of electrokinetic flow and transport in microfluidic chips. *Comput. Method. Appl. M.*, 198(30-32):2360 – 2367, 2009.
- Li D. *Electrokinetics in Microfluidics*. Elsevier Academic Press, 2004.
- MacInnes J.M. Computation of reacting electrokinetic flow in microchannel geometries. *Chem. Eng. Sci.*, 57(21):4539 – 4558, 2002.
- Patankar N. and Hu H. Numerical simulation of electroosmotic flow. *Anal. Chem.*, 70(9):1870–

- 1881, 1998.
- Peng Y., Pallandre A., Tran N.T., and Taverna M. Recent innovations in protein separation on microchips by electrophoretic methods. *Electrophoresis*, 29(1):157–178, 2008.
- Probstein R. *Physicochemical Hydrodynamics. An Introduction*. Wiley-Interscience, second edition, 2003.
- Saville D. and Palusinski O. Theory of electrophoretic separations. part i: Formulation of a mathematical model. *AIChE J.*, 32(2):207–214, 1986.
- Shim J., Dutta P., and Ivory C. Modeling and simulation of IEF in 2-D microgeometries. *Electrophoresis*, 28:572–586, 2007.
- Sounart T.L. and Baygents J.C. Lubrication theory for electro-osmotic flow in a non-uniform electrolyte. *J. Fluid. Mech.*, 576(-1):139–172, 2007.
- Tezduyar T., Mittal S., Ray S., and Shih R. Incompressible flow computations with stabilized bilinear and linear equal order interpolation velocity pressure elements. *Comput. Method. Appl. M.*, 95:221–242, 1992.
- Tezduyar T. and Osawa Y. Finite element stabilization parameters computed from element matrices and vectors. *Comput. Method. Appl. M.*, 190(3-4):411–430, 2000.
- Tezduyar T. and Senga M. Determination of the shock-capturing parameters in supg formulation of compressible flows. *Computational Mechanics WCCM IV, Beijing, China*, 2004, 2004.
- Thormann W., Caslavská J., and Mosher R. Modeling of electroosmotic and electrophoretic mobilization in capillary and microchip isoelectric focusing. *J. Chromatogr. A*, 1155(2):154 – 163, 2007.
- Tsai W.B., Hsieh C.J., and Chieng C.C. Parallel computation of electroosmotic flow in L-shaped microchannels. *6th World Congress of Structural and Multiisciplinary Optimization*, pages 4971–4980, 2005.
- Wu D., Qin J., and Lin B. Electrophoretic separations on microfluidic chips. *J. Chromatogr. A*, 1184(1-2):542 – 559, 2008.